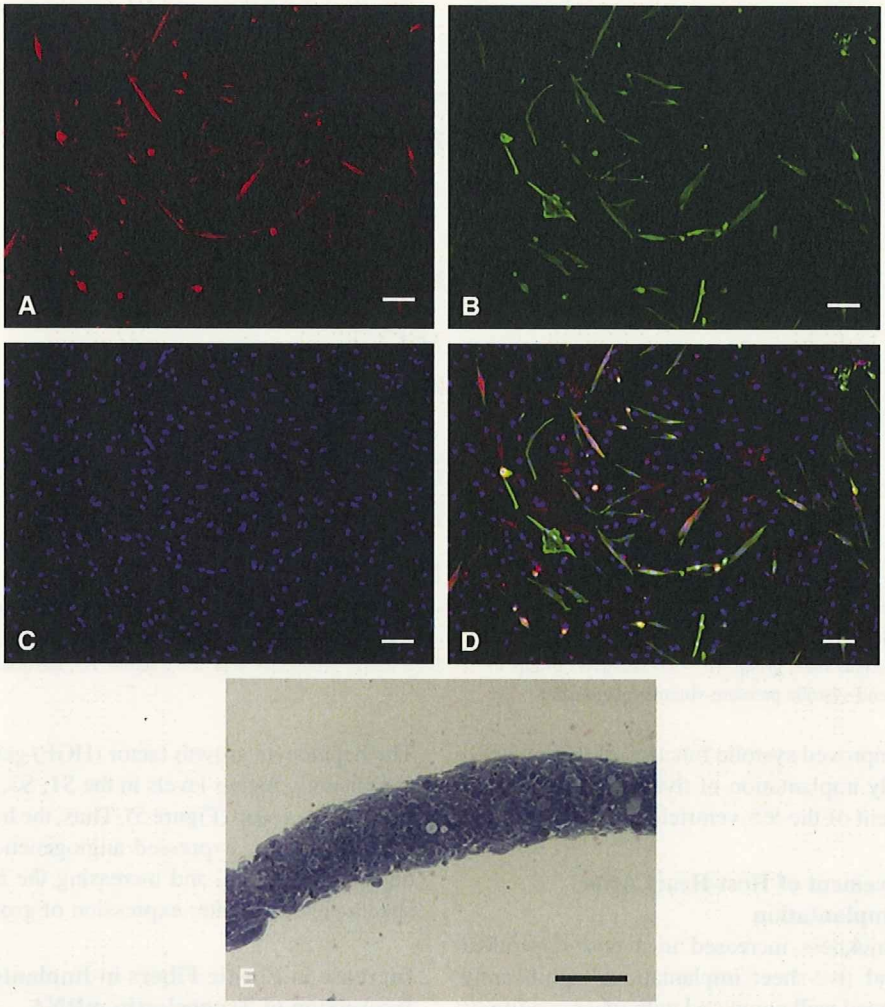

FIGURE 1. Cultured myoblasts and cross section of a sheet. Almost all cultured cells were actin-positive (A), and roughly 40% to 50% of them were desmin-positive muscle lineage cells (B). DAPI (4,6-diamino-2-phenylindole) staining of nuclei (C), and merged image (D) (A–D; magnification ×10, *bar* = 100 μm). Toluidine blue staining of cross section of sheet-constructed cells (E) (*bar* = 100 μm).

after implantation and immediately stored in RNA*later* solution (Qiagen, Hilden, Germany) until use (n = 10 for each of the 4 groups, S1, S3, S5, and sham). Total RNA was extracted with the RNeasy mini kit (Qiagen), and relative levels of mRNA transcripts were measured by the real-time quantitative reverse-transcriptase polymerase chain reaction (RT-PCR) technique using the ABI PRISM 7700 Sequence Detection System (Applied biosystems, Carlsbad, Calif).[18] The average copy number of gene transcripts in each sample was normalized to that for glyceraldehyde-3-phosphate dehydrogenase, and fold induction of each gene was calculated by the formula: Fold induction = Normalized value in a sample after MI/Mean of the normalized values for 15 reference myocardial samples.

Data Analyses

All values are the mean ± standard error of the mean. To assess the significance of differences between individual groups, we performed statistical evaluations with multiple analyses of variance. Differences in cardiac function data obtained by echocardiography were assessed by 2-way repeated-measures analysis of variance. If a significant F ratio was obtained, further analysis was carried out with a post hoc test.

RESULTS

Layered Myoblast Sheet Implantation Improved Cardiac Performance

Echocardiography revealed significant improvement of LV ejection fraction (LVEF) and percentage fractional shortening in the S3 and S5 groups compared with the S1 and sham groups 4 and 8 weeks after implantation. The LVEF 4 weeks after implantation in the S5 group was significantly improved compared with that in the S3 group ($P < .05$) (Figure 2, *A* and *B*). Enlargement of LV end-diastolic area was significantly attenuated in the S5 group compared with the sham and S1 groups at 4 weeks and differed significantly from the sham group 8 weeks after implantation (Figure 2, *C*). The end-systolic pressure–volume relationship was significantly improved in both the S3 and S5 groups compared with the S1 and sham groups 8 weeks after implantation (Figure 2, *D*). Thus, implantation of sheets of at

ET/BS

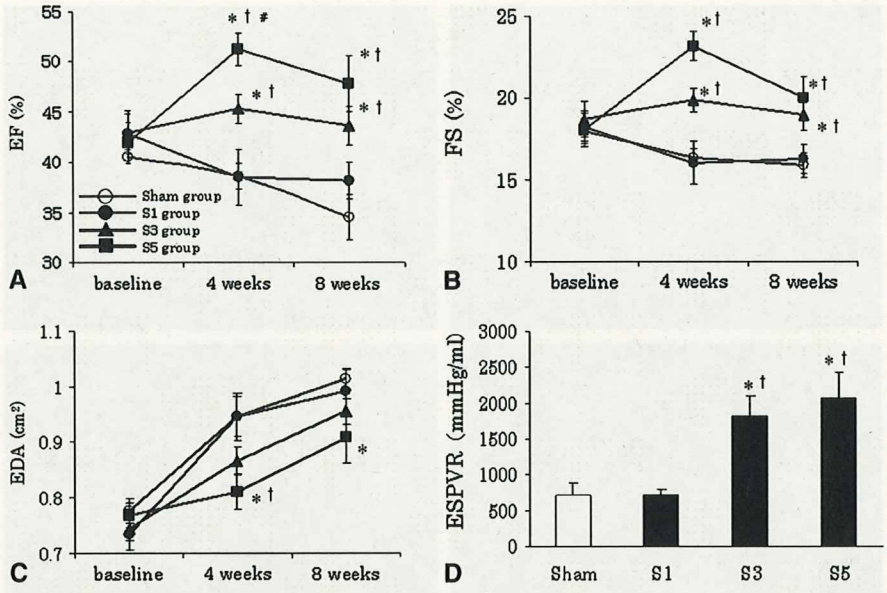

FIGURE 2. Cardiac function after layered myoblast sheet implantation. Echocardiographic measurements of rat heart (A–C). *Baseline* represents 2 weeks after left anterior descending coronary artery ligation. The pressure-volume study was performed at 8 weeks after treatment to estimate the systolic function of rat heart (D). *$P < .05$ versus sham group. †$P < .05$ versus S1 group. #$P < .05$ versus S3 group. *EF*, Ejection fraction; *FS*, fractional shortening; *EDA*, end-diastolic area; *ESPVR*, end-systolic pressure-volume relationship.

least three layers improved systolic function of the impaired heart, although only implantation of five-layered sheets attenuated enlargement of the left ventricle after infarction.

Histologic Improvement of Host Heart After Myoblast Sheet Implantation

Anterior wall thickness increased in a dose-dependent fashion. Three- and five-sheet implantations significantly thickened the infarcted wall compared with other conditions ($P < .05$) (Figure 3, *A* to *D*, and Figure 4, *A*). In the infarcted region 4 weeks after implantation, vascular density was significantly higher in the S3 and S5 groups than in the S1 and sham groups ($P < .05$). There was no significant difference in density between the S3 and S5 groups (Figure 3, *E* to *H*, and Figure 4, *B*). In noninfarcted regions at 4 weeks, picrosirius red staining revealed significant reduction of fibrosis in the S3 and S5 groups compared with the S1 and sham groups. The fibrosis in the S5 group was significantly reduced compared with that in the S3 group (Figure 3, *I* to *L*, and Figure 4, *C*). The mean diameters of the myocytes in the S3 and S5 groups were smaller than those in the S1 and sham groups ($P < .05$) (Figure 3, *M* to *P*, and Figure 4, *D*).

Assessment of Growth Factors by Gene Expression

RT-PCR analysis 4 weeks after implantation revealed significantly higher expression of stromal-derived factor 1 (SDF-1) in the S5 group than in the other groups ($P < .05$). Although expression of vascular endothelial growth factor (VEGF) increased in each group in a dose-dependent fashion, there were no significant differences among groups. The hepatocyte growth factor (HGF) gene was expressed to significantly higher levels in the S1, S3, and S5 groups than in the sham group (Figure 5). Thus, the hearts implanted with myoblast sheets expressed angiogenetic factors in a dose-dependent fashion, and increasing the number of myoblast sheets yielded greater expression of growth factors.

Increase in Elastic Fibers in Implanted Area With Expression of Tropoelastin mRNA

Masson's elastica staining showed that elastic fibers had increased not only in the implanted sheet layers but also in the infarcted scar area. In the S5 and S3 groups, the implanted sheets including elastic fibers surrounded the host heart over the infarcted area (Figure 6, *A* to *D*). In contrast, they were scarce in the S1 and sham groups (Figure 6, *E* and *F*). The relative expression of rat tropoelastin mRNA increased in a dose-dependent fashion. Expression in the S5 group was significantly higher than those in the sham and S1 groups ($P < .05$) (Figure 6, *G*).

DISCUSSION

In this study, we examined whether increasing the number of cell sheets used to attenuate cardiac remodeling and repair an infarcted myocardial wall improved cardiac performance. We found that implantation of five-layered myoblast sheets yielded favorable results, with improvement of cardiac function, induction of angiogenesis, less fibrosis, and less hypertrophy than the single-layered sheets used in this study or the two-layered sheets used in previous studies.[10,11] Sheet-shaped tissue maintains intact membrane and adhesive

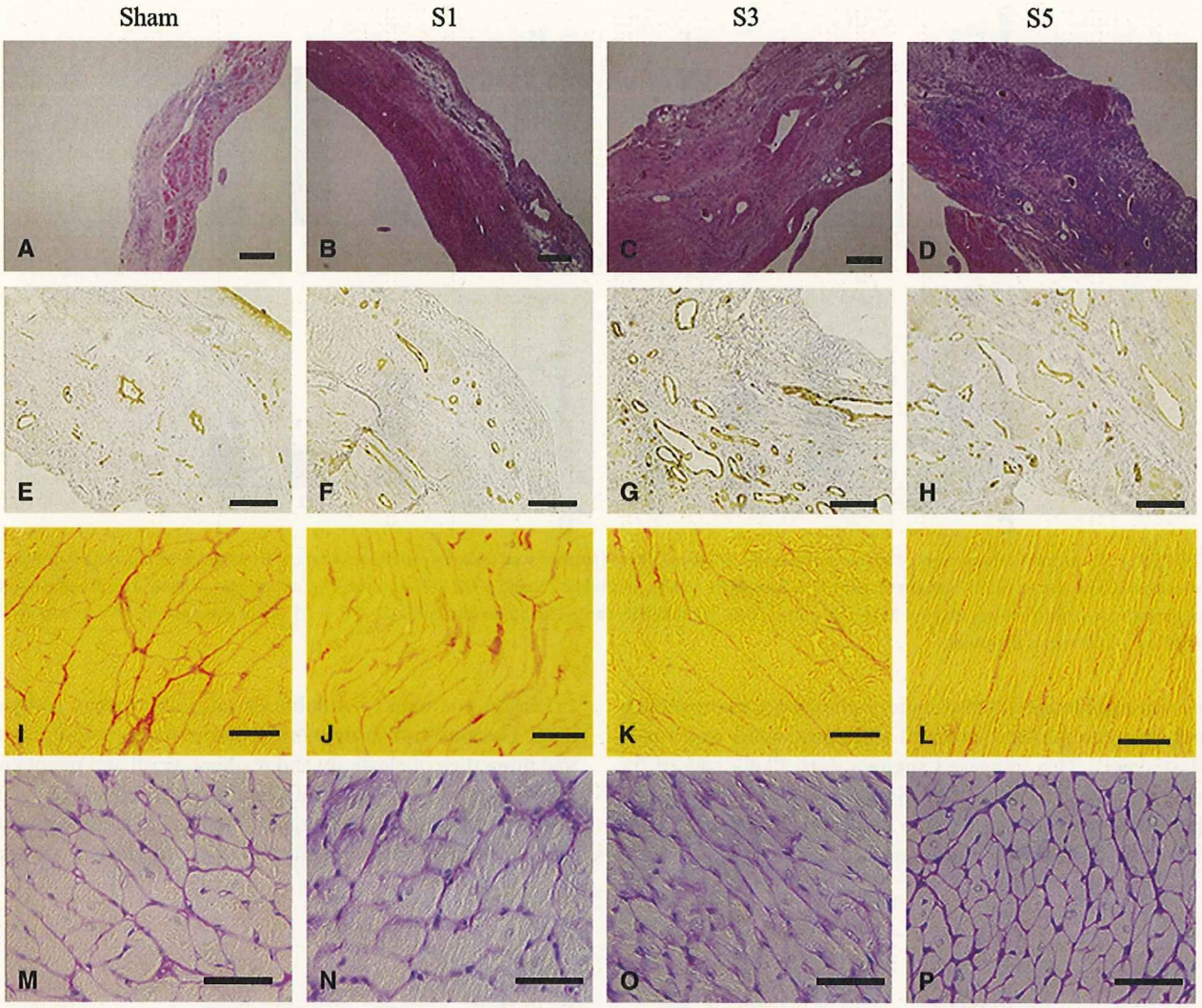

FIGURE 3. Histologic findings of implanted host hearts. Macroscopic (×20) view of anterior wall of hearts (hematoxylin and eosin stain): sham, A; S1, B; S3, C; S5, D (*bar* = 200 μm). Sections of infarcted regions were stained with antibody to von Willebrand factor (factor VIII): sham, E; S1l F; S3, G; S5, H (*bar* = 100 μm). Sirius-red staining of myocardium of noninfarcted regions: sham, I; S1, J; S3, K; S5, L (*bar* = 100 μm). Periodic acid–Schiff–stained myocardium of noninfarcted regions: sham, M; S1, N; S3, O; S5, P (*bar* = 50 μm).

proteins, incorporates extracellular matrix molecules, secretes growth factors owing to favorable cell-to-cell crosstalk, and prevents cellular microenvironment disruption by enzymatic reactions typically used to detach cells from tissue culture dishes (eg, trypsin or dispase).[19] These new tissue-engineered cell sheets are expected to be useful for cell delivery to the heart.[6,1,12]

Cardiac remodeling after MI appears to be compensatory initially, but has generally adverse effects and is linked to the progression of heart failure. Cardiomyocyte hypertrophy and interstitial fibrosis are usually observed in the remodeled heart, and greater ventricular enlargement correlates with a poorer prognosis for patients with coronary artery disease.[20,21] It is, therefore, now widely believed that ventricular remodeling is an important therapeutic target in patients with MI. Here, we treated MI hearts by implantation of layered myoblast sheets and observed decreased remodeling. The mechanism of this attenuation of remodeling may involve efficient delivery of myoblast sheets that overlap the scar area and its borders in the form of a cellular bridge.[11]

Expression of HGF, VEGF, and SDF-1 increases in the host heart implanted with myoblast sheets.[11] Therefore, layered myoblast sheets may be good suppliers of these factors for impaired hearts. HGF prevents the ventricular remodeling of hearts with established experimental MI.[22-25] Our previous findings suggested that SDF-1 is released from myoblasts, recruits hematopoietic stem cells, and facilitates repair of the infarcted heart. Similarly, the increased release of HGF and VEGF in the S3 and S5 treatment groups of the current study might have had advantageous effects in

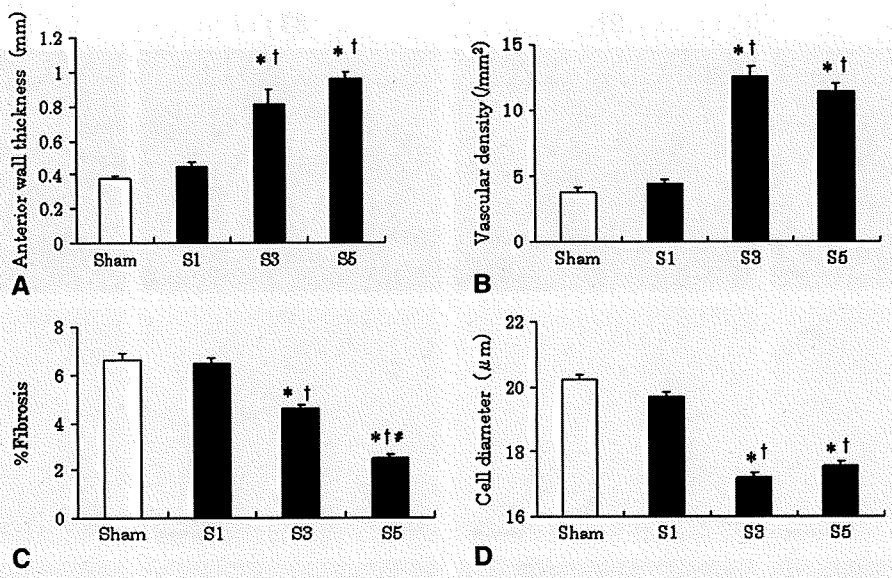

FIGURE 4. Quantitative assessment of histologic findings. A, Assessment of anterior wall thickness after implantation. B, Assessment of vascular density in the infarcted area of host hearts vascular density. C, Quantitative results for fibrotic change in the left ventricle. D, Cardiomyocyte short-axis diameters were measured as described in Methods (n = 5 for each group: A–D, 10 randomly chosen fields per section: B–D). *$P < .05$ versus sham group. †$P < .05$ versus S1 group. #$P <$. 05 versus S3 group.

the damaged heart. On histologic examination, microvessels were increased in the infarcted areas implanted with myoblast sheets. This increased angiogenesis, likely caused by increased HGF, VEGF, and SDF-1, may have improved the microenvironment of the myocytes, rescuing them from cell death or scar formation.

Elastin is a major insoluble extracellular matrix component. The elastic fiber network provides tissue with the critical properties of elasticity and resilient recoil and maintains the integrity of tissue architecture against repeated expansion.[26,27] Mizuno and colleagues[28] reported that transplantation of elastin gene–transfected cells attenuated adverse

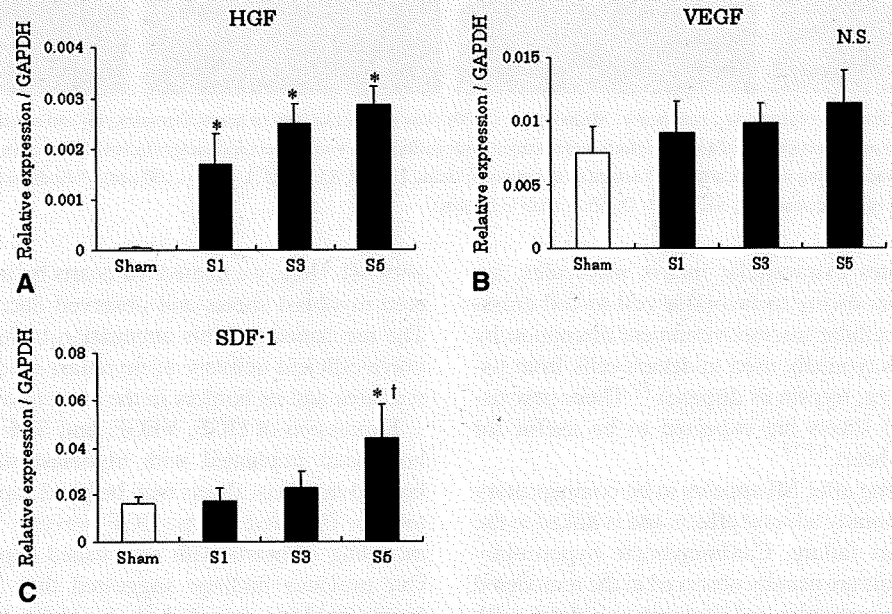

FIGURE 5. Relative expression of growth factors (A–C). Relative levels of mRNA transcripts were measured by the real-time quantitative RT-PCR (n = 10 for each of the four groups, S1, S3, S5, and sham). The average copy number of gene transcripts in each sample was normalized to that for glyceraldehyde-3-phosphate dehydrogenase *(GAPDH)*. *$P < .05$ versus sham group. †$P < .05$ versus S1 group. *HGF*, Hepatocyte growth factor; *VEGF*, vascular endothelial growth factor; *SDF-1*, stromal-derived factor-1.

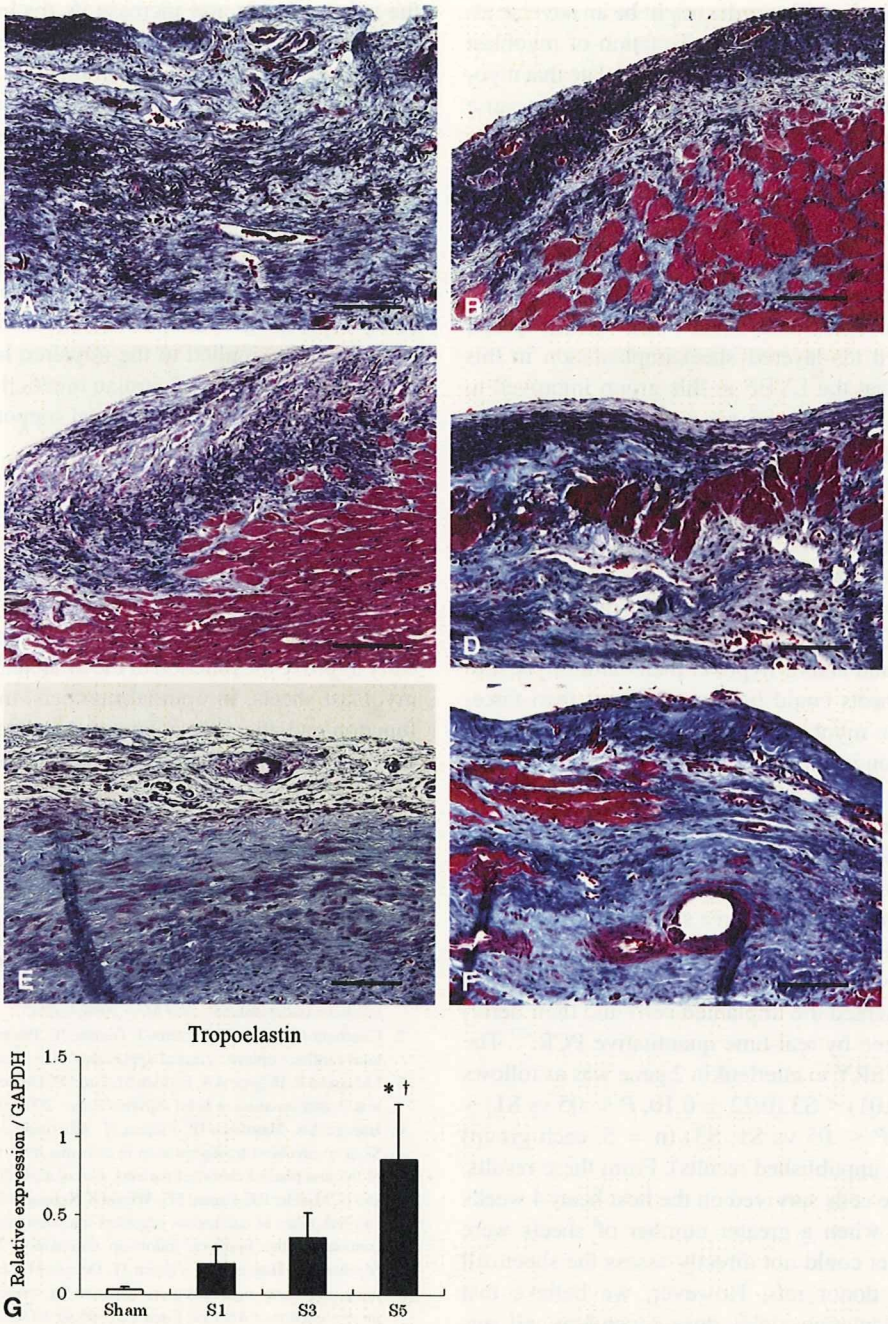

FIGURE 6. Elastic fibers were constructed after implantation, with expression of mRNA. Elastic fibers were increased in sheets and host infarcted area in the S5 and S3 groups (S5, A and B; S3, C and D). There were few elastic fibers in the S1 and sham groups (S1, E; sham, F). Relative expression of mRNA of tropoelastin (G). *$P < .05$ versus sham group. †$P < .05$ versus S1 group.

cardiac remodeling of the infarcted heart. The underlying mechanism may involve the addition of elasticity to the infarcted area, permitting recoil in response to the stresses of contraction, which might reduce scar thinning and dilatation. In our studies, implanted myoblast sheets organized elastic fibers not only in the sheet cells but also in the infarcted area of the host heart. Layered myoblast sheet cells might organize the elastic fibers within the cell sheets and infarcted area via expression of tropoelastin, which was expressed more strongly in the layered implantation groups (S3 and S5). It may thus provide elasticity to the host heart, with the improvement of systolic function and less LV dilatation.

We have never detected procedure-induced arrhythmia in these animal models.[11-13] Menasché and associates[6] reported

that sustained ventricular tachycardia might be an adverse effect after myoblast injection. The implantation of myoblast sheets seems to be safe in this regard. We speculate that myoblasts implanted into the heart may have the potential to cause random electrical activity, causing lethal arrhythmia. On the other hand, myoblast sheets implanted outside the epicardium may not generate sufficient aberrant electrical activity to cause lethal arrhythmia. Of course, this is speculation and further investigation, including electrophysiologic studies, is needed.

One of the limitations of this study is that implantation of more than five layers of myoblast sheets was not investigated. However, we tested ten-layered–sheet implantation in this model and found that the LVEF in this group improved to the same level as seen in the S5 group 4 and 8 weeks after implantation (Sekiya and Sawa; unpublished results). This suggests that improvement of cardiac function may plateau at five layers because of the insufficient supply of oxygen and nutrition for myoblasts. This contrasts with the study of Shimizu and associates,[14] who found that a maximum of three layers could be implanted at one time using cardiomyocyte sheets. Therefore, myoblasts may have a higher tolerance against ischemia and/or hypoxia than cardiomyocytes, and five-layered sheets could be more optimal than three-layered sheets when myoblast sheets are implanted.

Another limitation is of the current study is that the fate of the implanted cells was not tracked. We have begun addressing this by examining sheet cell survival 4 weeks after implantation. In brief, we transplanted male-derived cell sheets onto 15 female infarct hearts that were divided into three groups (S1, one sheet; S3, three sheets; S5, five sheets; n = 5 in each group). Four weeks later, genomic DNA was purified from the whole heart, and the male-specific SRY gene, which represented the implanted cells and their derivatives, was measured by real-time quantitative PCR.[29] The expression ratio of SRY to interleukin 2 gene was as follows (%): S1 (0.05 ± 0.01) < S3 (0.22 ± 0.10, $P < .05$ vs S1) < S5 (0.86 ± 0.16, $P < .05$ vs S1, S3) (n = 5, each group) (Sekiya and Sawa; unpublished results). From these results, we found that more cells survived on the host heart 4 weeks after implantation when a greater number of sheets were implanted. This fact could not directly assess the sheet cell survival on male donor rats. However, we believe that layered sheet implantation yields dose-dependent cell survival after implantation. Although we do not yet know the phenotype of these implanted cells, the survival data were compatible with the dose-dependent growth factor expression and increased wall thickness seen in the experiments presented here.

We propose the following mechanism of repair of the infarcted heart by layered myoblast sheets. At first, the implanted sheets might provide angiogenic and cardioprotective factors, such as HGF, VEGF, and SDF-1, to the host heart. These factors induce angiogenesis in the infarcted area. Additionally, the myoblast sheets mechanically cover the infarcted area and increase its thickness. Then, the implanted sheet cells express the elastin gene and form elastic fibers both in the sheets and in the host heart. The repaired heart, in turn, exhibits reduced wall stress, and LV dilatation, fibrosis, and hypertrophy are prevented.

Recently, we[30] have investigated 3-dimensional cell sheet construction in vitro using combinations of several different kinds of cells, such as endothelial cells and fibroblasts, aiming to induce vasculogenesis in cell sheets. In the future, beating cell sheets differentiated from pleuripotent stem cells, expressing connexin 43, and containing endothelial cells might be applied to the impaired heart and yield even greater improvement of cardiac function via different mechanisms, such as direct mechanical support through gap junctions, than those reported here.

In summary, our study demonstrated that implantation of myoblast sheets with five layers significantly improved LV systolic function for at least 2 months. Although the mechanism of this effect is not yet clear, a paracrine activity might induce angiogenesis and reduce fibrosis and hypertrophy. Elastic fibers in the cell sheets or host heart might mechanically improve the function of the infarcted heart. Thus, layered myoblast sheets, in optimal numbers, may improve cardiac function and attenuate adverse cardiac remodeling in the infarcted heart. A clinical trial is desired in the near future.

We thank Mrs Masako Yokoyama and Mr Kazuhiro Takekita for their excellent technical assistance and Dr Shannon L. Wyszomierski for correcting the grammar in the manuscript.

References

1. Taylor DA, Atkins BZ, Hungspreugs P, Jone TR, Reedy MC, Hutcheson KA, et al. Regenerating functional myocardium: improved performance after skeletal myoblast transplantation. *Nat Med.* 1998;4:929-33.
2. Chachques JC, Acar C, Herreros J, Trainini JC, Prosper F, D'Attellis N, et al. Cellular cardiomyoplasty: clinical application. *Ann Thorac Surg.* 2004;77:1121-3.
3. Menasché P, Hagege AA, Scorsin M, Puzet B, Desnos B, Schwartz K, et al. Myoblast transplantation in heart failure. *Lancet.* 2001;357:279-80.
4. Hagege AA, Marolleau JP, Vilqiun JT, Alheritiere A, Peyrard S, Duboc D, et al. Skeletal myoblast transplantation in ischemic heart failure: long-term follow-up of the first phase I cohort of patients. *Circulation.* 2006;114:I108-13.
5. Dib N, Michler RE, Pagani FD, Wright S, Kereiakes DJ, Lengerich R, et al. Safety and feasibility of autologous myoblast transplantation in patients with ischemic cardiomyopathy: four-year follow-up. *Circulation.* 2005;112:1748-55.
6. Menasché P, Hagege AA, Vilquin JT, Desnos M, Abergel E, Pouzet B, et al. Autologous skeletal myoblast transplantation for severe postinfarction left ventricular dysfunction. *J Am Coll Cardiol.* 2003;41:1078-83.
7. Pagani FD, DerSimonian H, Zawadzka A, Wetzel K, Edge AS, Jacoby DB, et al. Autologous skeletal myoblasts transplanted to ischemia-damaged myocardium in humans. Histological analysis of cell survival and differentiation. *J Am Coll Cardiol.* 2003;41:1078-83.
8. Suzuki K, Murtuza B, Fukushima S, Smolenski RT, Varela-Carver A, Coppen SR, et al. Targeted cell delivery into infarcted rat hearts by retrograde intracoronary infusion: distribution, dynamics, and influence on cardiac function. *Circulation.* 2004;110(Suppl II):II-225-30.
9. Okano T, Yamada N, Okuhara M, Sakai H, Sakurai Y. Mechanism of cell detachment from temperature-modulated, hydrophilic-hydrophobic polymer surfaces. *Biomaterials.* 1995;16:297-303.
10. Miyagawa S, Sawa Y, Kitagawa-Sakakida S, Taketani S, Kondoh H, Memon IA, et al. Tissue cardiomyoplasty using bioengineered contractile cardiomyocyte sheets to repair damaged myocardium: their integration with recipient myocardium. *Transplantation.* 2005;80:1586-95.

ET/BS

11. Memon IA, Sawa Y, Fukushima N, Matsumiya G, Miyagawa S, Taketani S, et al. Repair of impaired myocardium by means of implantation of engineered autologous myoblasts sheets. *J Thorac Cardiovasc Surg.* 2005;130:1333-41.
12. Kondoh H, Sawa Y, Miyagawa S, Sakakida-Kitagawa S, Memon IA, Kawaguchi N, et al. Longer preservation of cardiac performance by sheet-shaped myoblast implantation in dilated cardiomyopathy hamsters. *Cardiovasc Res.* 2005;69:466-75.
13. Hata H, Matsumiya G, Miyagawa S, Kondoh H, Kawaguchi N, Matsuura N, et al. Grafted skeletal myoblast sheets attenuate myocardial remodeling in pacing-induced canine heart failure model. *J Thorac Cardiovasc Surg.* 2006;132: 918-24.
14. Shimizu T, Sekine H, Yang J, Isoi Y, Yamato M, Kikuchi A, et al. Polysurgery of cell sheet grafts overcomes diffusion limits to produce thick, vascularized myocardial tissues. *FASEB J.* 2006;20:708-10.
15. Wiesman HF, Bush DE, Mannisi JA, Weisfeldt ML, Healy B. Cellular mechanism of myocardial infarct expansion. *Circulation.* 1988;78:186-201.
16. Nishio R, Sasayama S, Matsumori A. Left ventricular pressure–volume relationship in a murine model of congestive heart failure due to acute viral myocarditis. *J Am Coll Cardiol.* 2002;40:1506-14.
17. Lekgave ED, Kiriazis H, Zhao C, Xu Q, Moore XL, Su Y, et al. Relaxin reverses cardiac and renal fibrosis in spontaneously hypertensive rats. *Hypertension.* 2005; 46:412-8.
18. Horiguchi K, Sakakida-Kitagawa S, Sawa Y, Li ZZ, Fukushima N, Shirakura R, et al. Selective chemokine and receptor gene expressions in allografts that develop transplant vasculopathy. *J Heart Lung Trasnplant.* 2002;21: 1090-100.
19. Kushida A, Yamato M, Okano T, Kikuchi A, Sakurai Y, Okano T. Decrease in culture temperature releases monolayer endothelial cell sheets together with deposited fibronectin matrix from temperature-responsive culture surfaces. *J Biomed Mater Res.* 1999;45:355-62.
20. Sharpe N. Cardiac remodeling in coronary artery disease. *Am J Cardiol.* 2003; 93(suppl):17B-20B.
21. Opie LH, Commerford PJ, Gersh BJ, Pfeffer MA. Controversies in ventricular remodeling. *Lancet.* 2006;367:356-67.
22. Cittandini A, Grossman BA, Raffaele N, Katz S, Stromer H, Smith RJ, et al. Growth hormone attenuates early left ventricular remodeling and improves cardiac function in rats with large myocardial infarction. *J Am Coll Cardiol.* 1997;29:1109-16.
23. Li Y, Takemura G, Kosai K, Yuge K, Nagano S, Esaki M, et al. Postinfarction treatment with an adenoviral vector expressing hepatocyte growth factor relieves chronic left ventricular remodeling and dysfunction in mice. *Circulation.* 2003;107:2499-506.
24. Askari AT, Unzek S, Popovic ZB, Goldman CK, Torudi F, Penn MS, et al. Effect of stromal-cell–derived factor 1 on stem-cell homing and tissue regeneration in ischemic cardiomyopathy. *Lancet.* 2003;362:697-703.
25. Rarajczak MZ, Majaka M, Kucia M, Drukala J, Piper S, Janowska WA, et al. Expression of functional CXCR4 by muscle satellite cells and secretion of SDF-1 by muscle-derived fibroblasts is associated with the presence of both muscle progenitors in bone marrow and hematopoietic stem/progenitor cells in muscles. *Stem Cell.* 2003;21:363-71.
26. Kielty CM, Sherratt MJ, Shuttleworth CA. Elastic fibers. *J Cell Sci.* 2002;115: 2817-28.
27. Nakamura T, Lozano PR, Ikeda Y, Iwanaga Y, Hinek A, Minamisawa S, et al. Fibulin-5/DANCE is essential for elastogenesis in vivo. *Nature.* 2002;415:171-5.
28. Mizuno T, Terrence MY, Richard DW, Chris GK, Li R-K. Elastin stabilizes an infarct and preserves ventricular function. *Circulation.* 2005;112:I-81-8.
29. Kitagawa-Sakakida S, Tori M, Li Z, Horiguch K, Izutani H, Matsuda H, et al. Active cell migration in retransplanted rat cardiac allograft during the course of chronic rejection. *J Heart Lung Transplant.* 2000;19:584-90.
30. Tsuda Y, Shimizu T, Yamato M, Kikuchi A, Sasagawa T, Sekiya S, et al. Cellular control of tissue architectures using a three-dimensional tissue fabrication technique. *Biomaterials.* 2007;28:4939-46.

Skeletal myoblast sheet transplantation improves the diastolic function of a pressure-overloaded right heart

Takaya Hoashi, MD,[a] Goro Matsumiya, MD, PhD,[a] Shigeru Miyagawa, MD, PhD,[a] Hajime Ichikawa, MD, PhD,[a] Takayoshi Ueno, MD, PhD,[a] Masamichi Ono, MD, PhD,[a] Atsuhiro Saito, PhD,[a] Tatsuya Shimizu, MD, PhD,[b] Teruo Okano, MD, PhD,[b] Naomasa Kawaguchi, PhD,[c] Nariaki Matsuura, MD, PhD,[c] and Yoshiki Sawa, MD, PhD[a]

Objective: The development of right ventricular dysfunction has become a common problem after surgical repair of complex congenital heart disease. A recent study reported that tissue-engineered skeletal myoblast sheet transplantation improves left ventricular function in patients with dilated and ischemic cardiomyopathy. Therefore myoblast sheet transplantation might also improve ventricular performance in a rat model of a pressure-overloaded right ventricle.

Methods: Seven-week-old male Lewis rats underwent pulmonary artery banding. Four weeks after pulmonary artery banding, myoblast sheet transplantation to the right ventricle was performed in the myoblast sheet transplantation group (n = 20), whereas a sham operation was performed in the sham group (n = 20).

Results: Four weeks after performing the procedure, a hemodynamic assessment with a pressure–volume loop showed a compensatory increase in systolic function in both groups. However, only the myoblast sheet transplantation group showed a significant improvement in the diastolic function: end-diastolic pressure (sham vs myoblast sheet transplantation, 10.3 ± 3.1 vs 5.0 ± 3.7 mm Hg; $P < .001$), time constant of isovolumic relaxation (11.1 ± 2.5 vs 7.6 ± 1.2 ms, $P < .001$), and end-diastolic pressure–volume relationship (16.1 ± 4.5 vs 7.6 ± 2.4/mL, $P < .005$). The right ventricular weight and cell size similarly increased in both groups. A histologic assessment demonstrated significantly suppressed ventricular fibrosis and increased capillary density in the myoblast sheet transplantation group in comparison with those in the sham group. Reverse transcription–polymerase chain reaction demonstrated an increased myocardial gene expression of hepatocyte growth factor and vascular endothelial growth factor in the myoblast sheet transplantation group but not in the sham group.

Conclusions: Skeletal myoblast sheet transplantation improved the diastolic dysfunction and suppressed ventricular fibrosis with increased capillary density in a rat model of a pressure-overloaded right ventricle. This method might become a novel strategy for the myocardial regeneration of right ventricular failure in patients with congenital heart disease.

ET/BS

Because of recent developments in diagnostic methods, the establishment of new surgical techniques, and improvements in perioperative management, patients with complex congenital heart disease (CHD) are today often able to survive to adulthood. However, even after a successful repair, right ventricular (RV) overload remains in some patients, in whom it impairs RV function and influences long-term mortality and morbidity.[1-3] Chronic pressure overload is one of the major risk factors of RV dysfunction. In this situation the right ventricle is hypertrophied and systolic function is initially preserved, whereas diastolic function gradually deteriorates.[4,5] Prolonged exposure to excessive pressure overload results in irreversible RV failure. Clinically, the relationship between progressive fibrosis and RV function must be addressed.[6-8]

Recently, cardiac regeneration therapy has provided a new treatment for end-stage heart failure, and skeletal myoblasts are currently thought to be a potential cell source.[9-11] We developed a novel cell delivery system using temperature-responsive culture dishes,[12] and tissue-engineered cell sheets have been created without any scaffold, which maintains cell–cell interaction and extracellular matrix while avoiding any inflammatory reaction, and with improved cell survival.[13] Skeletal myoblast sheet transplantation (MST) has been shown to improve left ventricular (LV) contractility in several animal models of LV failure.[14-16] Otherwise, it is unclear whether MST can also affect the right ventricle, especially pressure-induced RV dysfunction. Hence this study assessed whether MST could improve RV function in rats after damage caused by pressure overload.

From the Department of Cardiovascular Surgery,[a] Osaka University Graduate School of Medicine, Osaka, Japan; the Institute of Advanced Biomedical Engineering and Science,[b] Tokyo Women's Medical University, Tokyo, Japan; and the Department of Molecular Pathology,[c] Osaka University Graduate School of Allied Health Science, Osaka, Japan.

Received for publication March 17, 2008; revisions received Oct 1, 2008; accepted for publication Feb 2, 2009.

Address for reprints: Yoshiki Sawa, MD, PhD, 2–2 Yamadaoka, Suita, Osaka 565-0871, Japan (E-mail: sawa@surg1.med.osaka-u.ac.jp).

J Thorac Cardiovasc Surg 2009;138:460-7
0022-5223/$36.00

doi:10.1016/j.jtcvs.2009.02.018

Abbreviations and Acronyms

BW = body weight
CFR = coronary flow reserve
EDPVR = end-diastolic pressure–volume relationship
Ees = end-systolic elastance
ESPVR = end-systolic pressure–volume relationship
GAPDH = glyceraldehyde-3-phosphate dehydrogenase
HGF = hepatocyte growth factor
IVS = intraventricular septum
LV = left ventricular
MS = myoblast cell sheet
MST = myoblast sheet transplantation
PA = pulmonary artery
PAB = pulmonary artery banding
PRSW = preload recruitable stroke work
RT-PCR = reverse transcription–polymerase chain reaction
RV = right ventricular
SW = stroke work
VEGF = vascular endothelial growth factor

MATERIALS AND METHODS

Animal Care

All experimental procedures and protocols used in this investigation were reviewed and approved by the institutional animal care and use committee and are in accordance with the National Institutes of Health "Guide for the care and use of laboratory animals" (National Institutes of Health publication no. 85-23, revised 1996).

Creation of Chronic RV Pressure Overload

A rat model of pulmonary artery banding (PAB) was established to create chronic RV pressure overload. Seven-week-old male Lewis rats (180–210 g) were anesthetized with an intraperitoneal injection of ketamine hydrochloride (50 mg/kg) and xylazine (5 mg/kg) and ventilated by using a volume-controlled respirator (2 mL, 60 cycles/min) with room air. A left thoracotomy was performed at the fourth intracostal space, and the main pulmonary artery (PA) was carefully exposed. As previously reported,[17] a 19-gauge injection needle (outer diameter, 1.1 mm) was placed alongside the PA, and a 3-0 polyester suture was tied tightly around the PA and the needle. Next, the needle was rapidly removed, and then a fixed diameter was set for the PA. Thereafter, the thorax was closed in layers, and the ventilator setting was changed (90 cycles/min) for half an hour to reduce the respiratory load.

Skeletal Myoblast Sheet Preparation

Creation of myoblast cell sheets (MSs) with temperature-responsive culture dishes (UpCell; Cellseed, Tokyo, Japan) was done according to previous reports.[14-16] Briefly, skeletal muscle was harvested from the hind legs of 4-week-old syngeneic rats. The purified myoblasts were incubated on 35-mm UpCell dishes at 37°C, with the cell numbers adjusted to 3×10^6 per dish. After 12 to 18 hours, the dishes were moved to a refrigerator set at 20°C and left there for 30 minutes. During that time, the MSs detached spontaneously from the surfaces. Each sheet measured from 10 to 15 mm in diameter.

Skeletal MST

Four weeks after PAB, a second left thoracotomy was performed at the fifth intracostal space after achievement of general anesthesia. After opening the pericardium, the RV anterior wall was exposed. Two MSs were grafted onto each anterior wall of the right ventricle in the MST group (n = 20), or a sham operation was performed in the sham group (n = 20). The pericardium was closed linearly before the thorax was closed to prevent the dislocation of MSs. In addition, age-matched rats that did not undergo surgical intervention were also prepared as a control group (n = 20).

Hemodynamic Study and Data Analysis

Four weeks after the MST or sham operation, 10 rats in each group were anesthetized and ventilated again and were set on the blanket warmer to maintain body temperature. A median sternotomy was performed, and the pericardium was opened carefully to minimize hemorrhaging. A silk thread was placed under the inferior vena cava just above the diaphragm to change the RV preload. After purse-string sutures were attached with 7-0 polypropylene, the conductance catheter (Unique Medical Co, Tokyo, Japan) was inserted through the RV apex toward the pulmonary valve along the longitudinal axis of the RV cavity and then fixed. A Miller 1.4F pressure-tip catheter (SPR-719; Millar Instruments, Houston, Tex) was also inserted from the RV anterior wall and fixed. For better volume measurement, a 1-mm curve was added to the original standard straight conductance catheter to fit the complex RV geometry. The position of the conductance catheter was determined by observing the pressure and segmental volume signals with the appropriate phase relationships. The conductance system and the pressure transducer controller (Integral 3 [VPR-1002], Unique Medical Co) were set as previously reported.[18] Pressure–volume loops and intracardiac electrocardiograms were monitored online, and the conductance, pressure, and intracardiac electrocardiographic signals were analyzed with Integral 3 software (Unique Medical Co).[18]

Under stable hemodynamic conditions, the baseline indices were initially measured, and then the pressure–volume loop was drawn during inferior vena caval occlusion and analyzed (Figure 1). Finally, the conductivity of the sampled blood was measured with a small (0.1 mm) cuvette, and the parallel conductance volume was measured with the hypertonic saline dilution method to obtain the absolute volumes.[19]

The following indices were calculated as the baseline RV function: heart rate, end-systolic pressure, end-diastolic pressure, dP/dtmax, dP/dtmin, and the time constant of isovolumic relaxation (τ). The following relationships were determined by means of pressure–volume loop analysis as load-independent measures of RV function: end-systolic pressure–volume relationship (ESPVR), end-diastolic pressure–volume relationship (EDPVR), and preload recruitable stroke work (PRSW).

The ESPVR is linear, and it can be characterized by a slope (end-systolic elastance [Ees]) and a volume axis intercept (Vo), so that $Pes = Ees(Ves–Vo)$, where Pes and Ves are the end-systolic pressure and volume, respectively.[20]

In contrast, the EDPVR is intrinsically thought to be nonlinear. The relationship between the end-diastolic pressure (Ped) and volume (Ved) can be fitted to the monoexponential, so that $Ped = Po+be^{KvVed}$, where Po is the pressure asymptote (generally close to 0 mm Hg), b is a constant, and Kv is the variable represented as a ventricular stiffness property.[21]

The relationship between ventricular stroke work (SW) and end-diastolic volume (Ved) is represented as PRSW. PRSW is thought to be a suitable parameter of the contractile state and fitted to the following equation: $SW = K(Ved–Vo)$, where K is a constant as a potential measure of intrinsic myocardial performance independent of loading, geometry, and heart rate.[22]

Histopathologic Analysis

The other 10 rats in each group were killed 4 weeks after the sham or MST operation for histologic analysis, reverse transcription–polymerase chain reaction (RT-PCR), and blood sampling. The hearts were quickly removed, and the ventricles were dissected free of atrial tissue and large

ET/BS

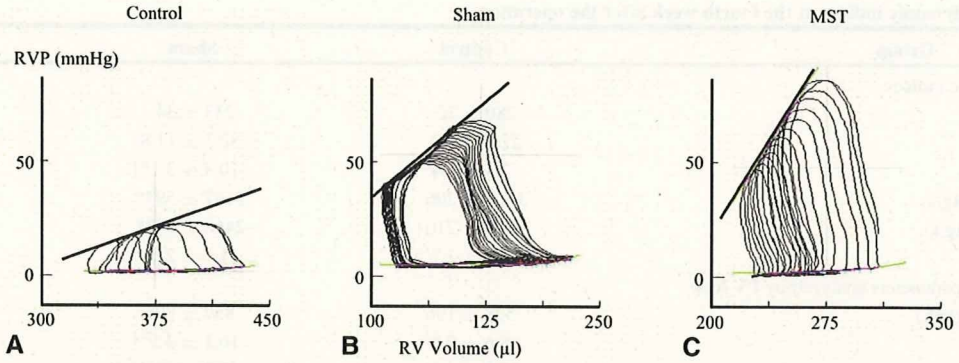

FIGURE 1. Representative pressure–volume loops of the control (A), sham (B), and myoblast sheet transplantation (*MST*; C) groups under different loading conditions. The slope of the end-systolic pressure–volume relationship is displayed as a *black straight line*. The correlation of the end-diastolic pressure–volume relationship is displayed as a *green monoexponential curve*. *RVP*, Right ventricular pressure; *RV*, right ventricle.

blood vessels. The right ventricle was carefully separated from the left ventricle and intraventricular septum (IVS). The fresh ventricular tissues were immediately blotted dry and weighted separately to determine the degree of RV hypertrophy based on 2 parameters: RV wall weight/body weight (RV/BW) and RV wall weight/LV and IVS wall weight (RV/LV+IVS).

Tissue specimens were obtained from the endocardium, the midwall, and the epicardium of the RV anterior wall in cross-sections, cut into 5-μm-thick sections, and stained with hematoxylin and eosin for morphologic analysis, including measurement of RV wall thickness, periodic acid–Schiff staining to measure the short-axis length of the RV myocardial cell, Factor VIII–related antigen staining (Dako EPOS anti-human Von Willebrand factor/HRP; Dako Cytomation, Glostrup, Denmark) to quantify capillary vascular density, and Masson trichrome staining for determination of the amount of interstitial and myocardial fibrosis. The percentage of interstitial and myocardial fibrosis were assessed by a computer-based method[23,24] with the use of a software filter (Mac Scope Software; MITANI Corp, Tokyo, Japan), which can recognize the distinct color shades. The number of pixels of the blue-stained collagen area was calculated, then divided by the total number of pixels in a field. Each 3 fields of the endocardial, epicardial, and mid layers of the RV wall per slide were analyzed and then averaged.

RT-PCR

Total RNA was isolated from the stored specimens by using the RNeasy Mini Kit (Qiagen, Hilden, Germany) and reverse transcribed with Omniscript Reverse Transcriptase (Qiagen). RT-PCR was performed with the ABI PRISM 7700 (Applied Biosystems, Foster City, Calif). Measurement of the mRNA expression of hepatocyte growth factor (HGF) and vascular endothelial growth factor (VEGF) was performed in triplicate. The results are expressed after normalization for glyceraldehyde-3-phosphate dehydrogenase (GAPDH).

Statistical Analysis

All data were expressed as the mean ± SEM and range. Student's unpaired *t* test or analysis of variance for parametric values was used to compare group means.

RESULTS

Pressure Overload and Hypertrophy of the Right Ventricle After PAB

After PAB, a weight analysis showed the heart weight/BW, RV/BW, and RV/(LV+IVS) weight ratios in the sham and MST groups to be similar and significantly higher than in the control group (Table 1). Both the sham and MST groups showed a significantly increased end-systolic pressure and dP/dtmax than seen in the control group (Table 2).

Hemodynamic Effects of MST

The baseline indices revealed that end-diastolic pressure and τ values were significantly increased only in the sham group in comparison with those in the control group but not in the MST group (Table 2). Typical examples of the pressure–volume loop in each group are presented in Figure 1. The pressure–volume loop analysis revealed that the ESPVR and PRSW values significantly increased both in the sham and MST groups. However, the EDPVR value significantly increased only in the sham group (control vs sham vs MST groups: 8.6 ± 2.9 vs 16.1 ± 4.5 vs 7.6 ± 2.4/mL; $P < .05$ in the control and MST groups vs the sham group; Table 2).

Histologic Effects of MST

Whole heart findings showed the RV wall thickened, the cavity enlarged, and the IVS shifted toward the left side in the sham and MST groups (Figure 2, *A*). In the MST group transplanted MSs were observed as an elastic thin layer on the epicardium (Figure 2, *B*). The RV wall thickness and myocardial cell size in the sham and MST groups were similar and significantly higher than in the control group (Figure 2, *C–E*).

TABLE 1. Weight analysis at the fourth week after the operation

Group	Control	Sham	MST
HW/BW (mg/g)	2.62 ± 0.09	3.53 ± 0.50*	4.03 ± 0.59*
RV/BW (mg/g)	0.54 ± 0.15	1.62 ± 0.42*	1.65 ± 0.32*
RV/(IVS+LV)	0.27 ± 0.08	0.69 ± 0.11*	0.69 ± 0.09*

MST, Myoblast sheet transplantation; *HW*, heart weight; *BW*, body weight; *RV*, right ventricle; *IVS*, interventricular septum; *LV*, left ventricle. *$P < .05$ versus the control group.

TABLE 2. Hemodynamic indices at the fourth week after the operation

Group	Control	Sham	MST
Basic hemodynamic indices			
HR (beats/min)	280 ± 72	233 ± 34	249 ± 65
ESP (mm Hg)	22.8 ± 2.9	82.3 ± 11.8*	78.7 ± 13.2*
EDP (mm Hg)	2.4 ± 1.4	10.3 ± 3.1*†	5.0 ± 3.7
dP/dtmax (mm Hg/s)	1301 ± 206	3197 ± 597*	3352 ± 1332*
dP/dtmin (mm Hg/s)	–997 ± 210	–2466 ± 582*	–2682 ± 828*
τ (ms)	7.9 ± 2.7	11.1 ± 2.5*†	7.6 ± 1.2
Load-independent parameters analyzed by PV loop			
ESPVR (mm Hg/mL)	538 ± 196	857 ± 305*	967 ± 201*
EDPVR (/mL)	8.6 ± 2.9	16.1 ± 4.5*†	7.6 ± 2.4
PRSW (mm Hg)	17.0 ± 4.1	40.2 ± 19.6*	40.8 ± 13.6*
PRSW/RV (mm Hg/kg)	88.3 ± 23.9	71.5 ± 31.3	73.6 ± 28.8

MST, Myoblast sheet transplantation; *HR*, heart rate; *ESP*, end-systolic pressure; *EDP*, end-diastolic pressure; *PV*, pressure–volume; *ESPVR*, end-systolic pressure–volume relationship; *EDPVR*, end-diastolic pressure–volume relationship; *PRSW*, preload-recruitable stroke work; *RV*, right ventricular weight. *P < .05 versus the control group. †P < .05 versus the MST group.

Factor VIII stain showed that myocardial capillary vascular density showed no significant difference at the mid layer and endocardial layer (Figure 3, *B* and *C*), but it was significantly higher in the MST group than in the other 2 groups at the epicardial layer (Figure 3, *A*). Hence, total capillary density in the MST group was significantly higher than in the other 2 groups (control vs sham vs MST groups: 262 ± 98 vs 271 ± 289 vs 823 ± 708; P <0.05 in the control and sham groups vs the MST group; Figure 3, *D*).

Periodic acid–Schiff staining demonstrated significant interstitial fibrosis of the right ventricle in both the sham and MST groups, but the percentage of fibrosis in the

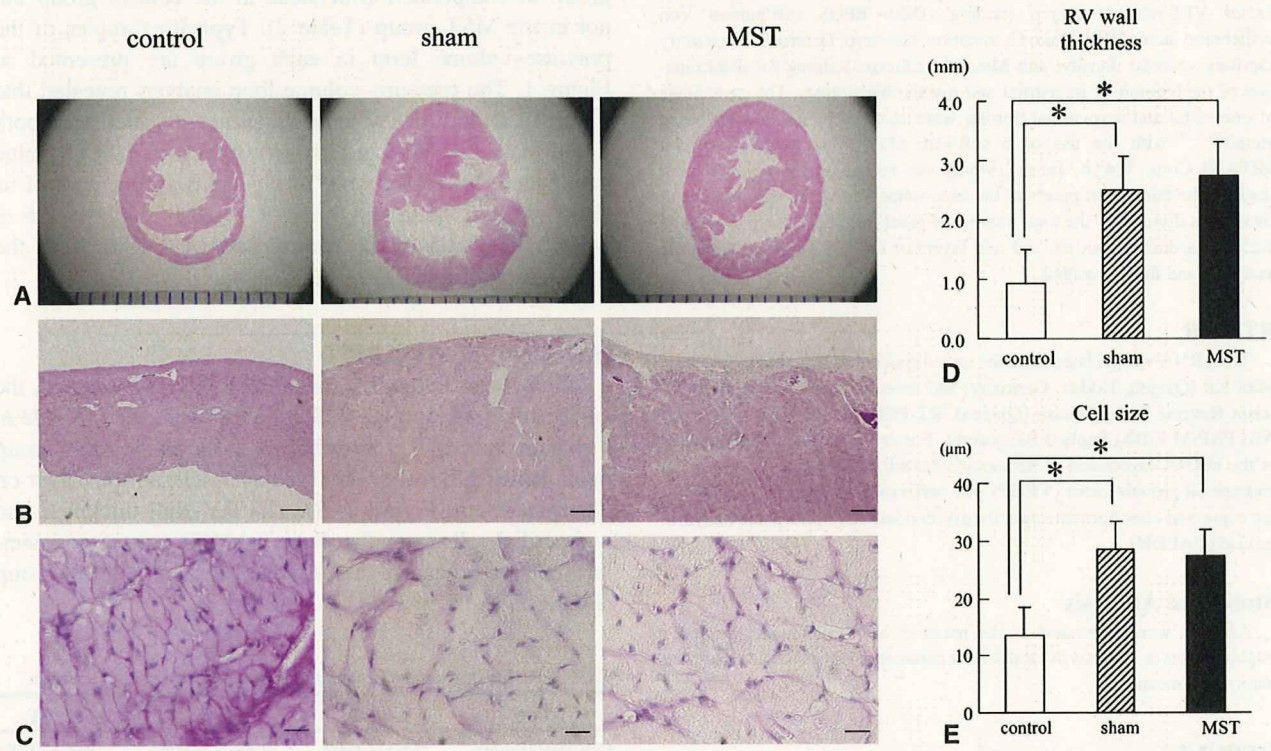

FIGURE 2. Macroscopic photographs of hematoxylin and eosin–stained sections showing right ventricular *(RV)* wall thickening, cavity enlarging, and the intraventricular septum shifting towered the left side in the sham and myoblast sheet transplantation *(MST)* groups (A and D). Photomicrographs (40×, scale bar = 200 μm) of hematoxylin and eosin–stained sections showed a fibrous organized thin layer on the epicardium in the myoblast sheet transplantation group (B). Photomicrographs (400×, scale bar = 20 μm) of periodic acid–Schiff–stained sections showed significantly hypertrophied ventricular myocytes in the sham and myoblast sheet transplantation groups (C and E). *P < .05 (n = 10).

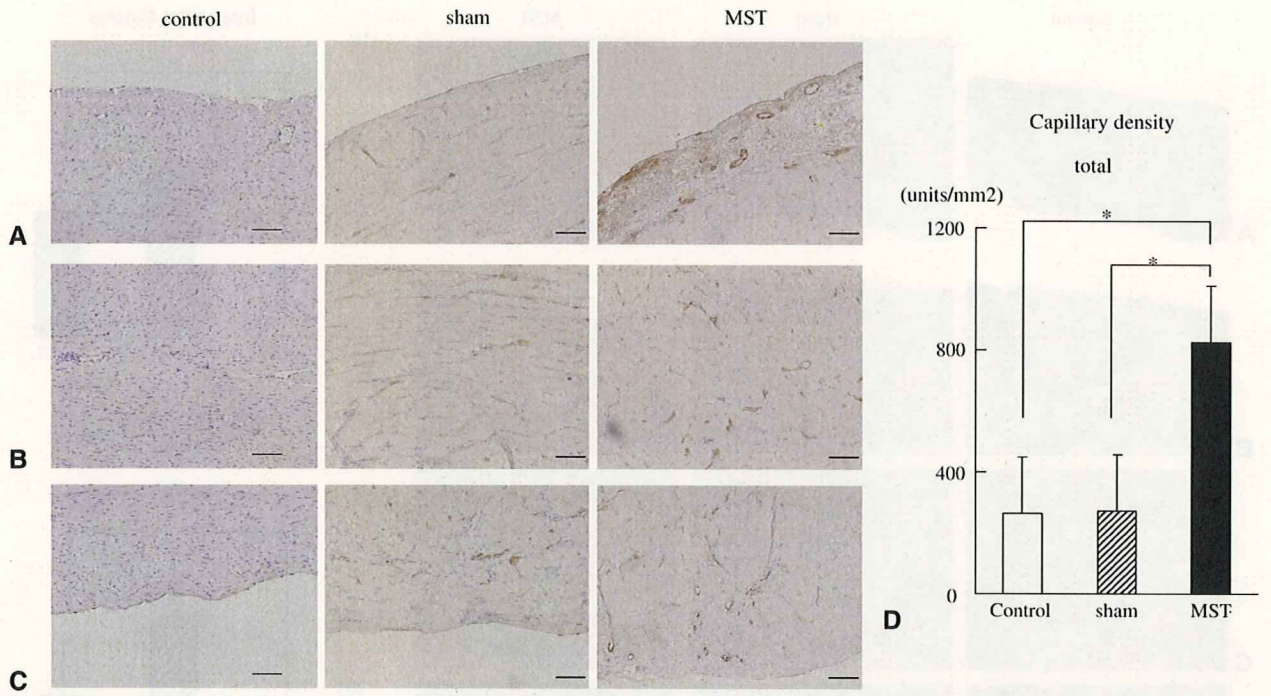

FIGURE 3. Representative photomicrographs (100×, scale bar = 100 μm) of Factor VIII–stained epicardial layer (A), mid layer (B), and endocardial layer (C). Neovascularization occurred at the epicardial layer in the myoblast sheet transplantation *(MST)* group (D). *$P < .05$ (n = 10).

MST group was significantly less than that in the sham group (control vs sham vs MST groups: 4.8% ± 1.1% vs 24.5% ± 10.0% vs 19.0% ± 5.1%; $P < .05$ between each 2 groups; Figure 4, *A* and *E*). Aggregated endomyocardial fibrosis was detected only in the sham group (endomyocardial percentage of fibrosis, control vs sham vs MST groups: 5.7% ± 0.1% vs 31.5% ± 8.4% vs 18.6% ± 5.9%; $P < .01$ in the control and MST groups vs the sham group; Figure 4, *B–D* and *F*).

RT-PCR

The expression of HGF and VEGF mRNA in the MST group was significantly higher than in the sham group (control vs sham vs MST groups: HGF, 0.00009 ± 0.00008 vs 0.00041 ± 0.00030 vs 0.00073 ± 0.00031/GAPDH [$P < .05$ in each group]; *VEGF*, 0.00242 ± 0.00164 vs 0.00329 ± 0.00181 vs 0.00512 ± 0.00113/GAPDH [$P < .05$ in the control and sham group vs the MST group]; Figure 5).

DISCUSSION

This study demonstrated that skeletal MST improved diastolic function in a pressure-overloaded right heart model in rats by means of PAB. This conclusion is supported by the following evidence: (1) the diastolic function was significantly improved based on hemodynamic assessment and pressure–volume loop analysis; (2) interstitial and endocardial fibrosis was ameliorated, and capillary vascular density of the epicardial layer was increased; and (3) myocardial gene expression of HGF and VEGF was significantly increased. MST has been shown to have therapeutic effects in several models of LV failure.[14-16] However, the present results are the first to show evidence that MST is effective for the treatment of RV dysfunction resulting from chronic pressure overload.

Prolonged RV pressure overload promotes unique morphologic, histologic, and functional changes. The mechanical stimulation of pressure overload extends the myocardium, which leads to diastolic dysfunction.[21] Simultaneously, hypertrophied myocardium upregulates the release of various chemical mediators,[17] which induce further myocardial expansion, apoptosis, necrosis, and fibrosis, finally resulting in RV decompensation. Otherwise, ventricular hypertrophy itself reduces the coronary flow reserve (CFR) and leads to coronary microcirculatory dysfunction.[25] As studies on the left ventricle show, this phenomenon is detected particularly in the subendocardium.[26] The shortage of CFR induces myocardial cellar mortality and endocardial fibrosis, which accelerates ventricular dysfunction. The present and previous data indicate that transplanted elastic cells initially improved ventricular stiffness[14] and preserved CFR in the hypertrophied myocardium, both of which generate a synergistic effect of the suppression of myocardial cell death and fibrosis, especially at the endocardial layer. Although an angiogenetic effect was observed with the increased myocardial gene expression of HGF and VEGF, we speculate this does not increase endocardial coronary flow directly because increased

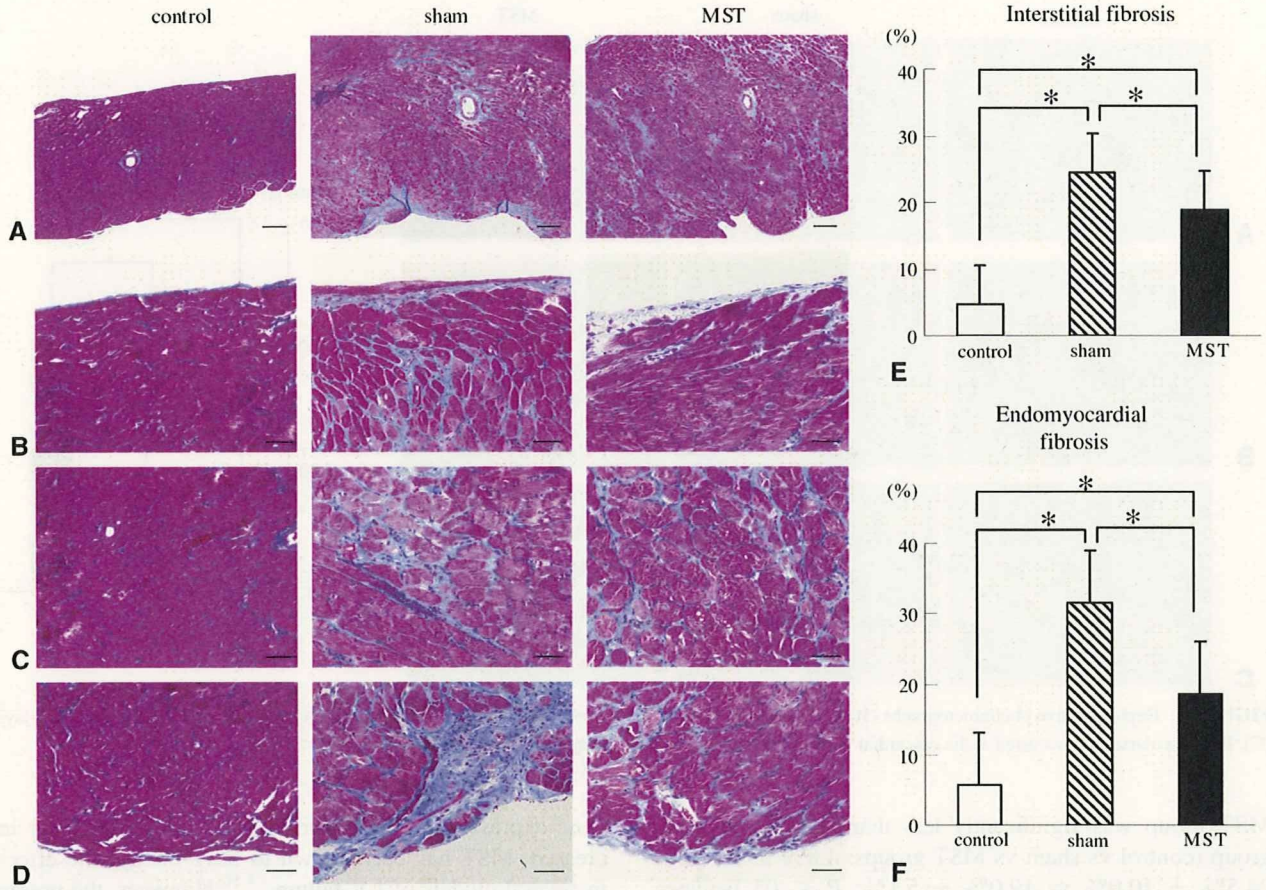

FIGURE 4. Representative photomicrographs of Masson's trichrome–stained transmural layer (A; 40×, scale bar = 200 μm), epicardial layer (B), mid layer (C), and endocardial layer (D; 200×, scale bar = 50 μm) for evaluation of interstitial (E) and endomyocardial (F) fibrosis. *$P < .05$ (n = 10).

capillary density was only seen at epicardial layer. These new capillaries might increase the blood supply to the transplanted myoblasts and prolong their survival.[13]

As several LV studies have previously shown, Lamberts and colleagues[27] revealed the strict relationship between RV chamber stiffness and the degree of myocardial fibrosis. In their report they also described that prevention or reduction of RV fibrosis improved RV diastolic dysfunction. Although we could not show any individual correlation between collagen contents and hemodynamic parameters in regard to diastolic function, these findings strongly support our results. Therefore we would like to emphasize that the suppression of fibrosis improved the RV diastolic function.

The hemodynamic assessment of cardiac performance of a hypertrophied right ventricle has not been established. Various attempts have been made; however, it is still necessary to perform cardiac catheterization to evaluate hemodynamics, especially regarding diastolic function.[28,29] Leeuwenburgh and associates[4] showed that RV compliance deteriorated in a lamb model and described τ and EDPVR values to be useful indicators for diastolic function. Gaynor

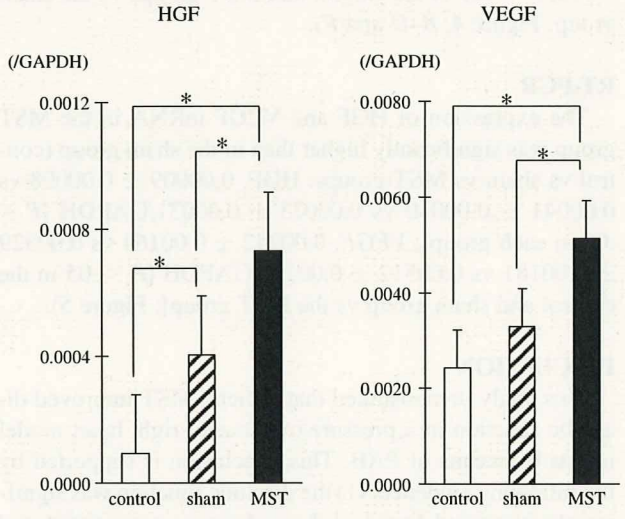

FIGURE 5. RT-PCR for evaluation of neurohormonal factor gene expression. The results are expressed after normalization for GAPDH. *HGF*, Hepatocyte growth factor; *VEGF*, vascular endothelial growth factor. *$P < .05$ (n = 10).

and coworkers[5] also showed an increase of EDPVR in a dog model of PAB. The current results are consistent with these reports. Therefore these data appear to be reliable.

On the other hand, the assessment of systolic function still remains controversial. In this study we showed that ESPVR (Ees) and PRSW were significantly increased in sham groups, as previously reported.[30] However, Dell'Italia and Walsh[31] pointed out that in the assessment of RV contractility, the slope of ESPVR (Ees) was different from the slope of the maximum time-varying elastance, which better reflected the RV contractility than Ees. In addition to Ees, PRSW is thought to be an optimal parameter of ventricular contractility. However, we might have to consider the discrepancy of the cardiac mass between normal and hypertrophied hearts because ventricular SW should be assessed as a per-unit cardiac mass. We tried to calculate the PRSW divided for each animal's RV weight, which revealed there was no statistical significance among the 3 groups (control vs sham vs MST groups: 88.3 ± 23.9 vs 71.5 ± 31.3 vs 73.6 ± 28.8 mm Hg/kg, Table 2). Hence it is hard to say that the RV pressure load induced a further improvement in RV contractility.

We need further investigation to apply this method to clinical RV failure because we did not ascertain the effect of MST on RV systolic function. Nevertheless, enormous fibrosis was seen in the sham group, and systolic function was still compensated until the timing of hemodynamic evaluation. However, previous reports showed that MST had an excellent effect on LV contractility.[14-16] Therefore we expect that this method might become a novel and potentially effective treatment strategy for patients with RV failure.

In conclusion, chronic pressure overload to the right ventricle caused hypertrophy and impaired diastolic function in rats. Skeletal MST attenuated diastolic dysfunction, which was mainly caused by suppressed interstitial and endocardial fibrosis. This method might become a novel strategy for the myocardial regeneration of RV failure in patients with CHD in the future.

We thank Mrs Masako Yokoyama for her expert assistance with RT-PCR and Kazuhiro Takekita and Takeshi Miki for technical support in creating the tissue-engineered skeletal MSs.

References

1. Bolger AP, Coats AJ, Gatzoulis MA. Congenital heart disease: the original heart failure syndrome. *Eur Heart J*. 2003;24:970-6.
2. Murphy JG, Gersh BJ, Mair DD, Fuster V, McGoon MD, Ilstrup DM, et al. Long-term outcome in patients undergoing surgical repair of tetralogy of Fallot. *N Engl J Med*. 1993;329:593-9.
3. Gatzoulis MA, Balaji S, Webber SA, Siu SC, Hokanson JS, Poile C, et al. Risk factors for arrhythmia and sudden cardiac death late after repair of tetralogy of Fallot: a multicentre study. *Lancet*. 2000;356:975-81.
4. Leeuwenburgh BP, Steendijk P, Helbing WA, Baan J. Indexes of diastolic RV function: load dependence and changes after chronic RV pressure overload in lambs. *Am J Physiol Heart Circ Physiol*. 2002;282:1350-8.
5. Gaynor SL, Maniar HS, Bloch JB, Steendijk P, Moon MR. Right atrial and ventricular adaptation to chronic right ventricular pressure overload. *Circulation*. 2005;112:212-8.
6. Deanfield JE, Ho SY, Anderson RH, McKenna WJ, Allwork SP, Hallidie-Smith KA. Late sudden death after repair of tetralogy of Fallot: a clinicopathologic study. *Circulation*. 1983;67:626-31.
7. Babu-Narayan SV, Kilner PJ, Li W, Moon JC, Goktekin O, Davlouros PA, et al. Ventricular fibrosis suggested by cardiovascular magnetic resonance in adults with repaired tetralogy of Fallot and its relationship to adverse markers of clinical outcome. *Circulation*. 2006;113:405-13.
8. Chowdhury UK, Sathia S, Ray R, Singh R, Pradeep KK, Venugopal P. Histopathology of the right ventricular outflow tract and its relationship to clinical outcomes and arrhythmias in patients with tetralogy of Fallot. *J Thorac Cardiovasc Surg*. 2006;132:270-7.
9. Taylor DA, Atkins BZ, Hungspreugs P, Jones TR, Reedy MC, Hutcheson KA, et al. Regenerating functional myocardium: improved performance after skeletal myoblast transplantation. *Nat Med*. 1998;4:929-33.
10. Menasche P, Hagege AA, Scorsin M, Pouzet B, Desnos M, Duboc D, et al. Myoblast transplantation for heart failure. *Lancet*. 2001;357:279-80.
11. Hagege AA, Marolleau JP, Vilquin JT, Alheritiere A, Peyrard S, Duboc D, et al. Skeletal myoblast transplantation in ischemic heart failure: long-term follow-up of the first phase I cohort of patients. *Circulation*. 2006;114:108-13.
12. Okano T, Yamada N, Sakai H, Sakurai Y. A novel recovery system for cultured cells using plasma-treated polystyrene dishes grafted with poly(N-isopropylacrylamide). *J Biomed Mater Res*: 1993;27:1243-51.
13. Miyagawa S, Sawa Y, Sakakida S, Taketani S, Kondoh H, Memon IA, et al. Tissue cardiomyoplasty using bioengineered contractile cardiomyocyte sheets to repair damaged myocardium: their integration with recipient myocardium. *Transplantation*. 2005;80:1586-95.
14. Memon IA, Sawa Y, Fukushima N, Matsumiya G, Miyagawa S, Taketani S, et al. Repair of impaired myocardium by means of implantation of engineered autologous myoblast sheets. *J Thorac Cardiovasc Surg*. 2005;130:1333-41.
15. Kondoh H, Sawa Y, Miyagawa S, Sakakida-Kitagawa S, Memon IA, Kawaguchi N, et al. Longer preservation of cardiac performance by sheet-shaped myoblast implantation in dilated cardiomyopathic hamsters. *Cardiovasc Res*. 2006;69:466-75.
16. Hata H, Matsumiya G, Miyagawa S, Kondoh H, Kawaguchi N, Matsuura N, et al. Grafted skeletal myoblast sheets attenuate myocardial remodeling in pacing-induced canine heart failure model. *J Thorac Cardiovasc Surg*. 2006;132:918-24.
17. Lekanne Deprez RH, van den Hoff MJ, de Boer PA, Ruijter PM, Maas AA, Chamuleau RA, et al. Changing patterns of gene expression in the pulmonary trunk-banded rat heart. *J Mol Cell Cardiol*. 1998;30:1877-88.
18. Sato T, Shishido T, Kawada T, Miyano H, Miyashita H, Inagaki M, et al. ESPVR of in situ rat left ventricle shows contractility-dependent curvilinearity. *Am J Physiol Heart Circ Physiol*. 1998;274:H1429-34.
19. Baan J, van der Velde ET, de Bruin HG, Smeenk GJ, Koops J, van Dijk AD, et al. Continuous measurement of left ventricular volume in animals and humans by conductance catheter. *Circulation*. 1984;70:812-23.
20. Suga H, Sagawa K. Instantaneous pressure-volume relationships and their ratio in the excised, supported canine left ventricle. *Circ Res*. 1974;35:117-26.
21. Gaasch WH, Cole JS, Quinones MA, Alexander JK. Dynamic determinants of left ventricular diastolic pressure-volume relations in man. *Circulation*. 1975;51:317-23.
22. Glower DD, Spratt JA, Snow ND, Kabas JS, Davis JW, Olsen CO, et al. Linearity of the Frank-Starling relationship in the intact heart: the concept of preload recruitable stroke work. *Circulation*. 1985;71:994-1009.
23. Hoyt RH, Collins SM, Skorton DJ, Ericksen EE, Conyers D. Assessment of fibrosis in infarcted human hearts by analysis of ultrasonic backscatter. *Circulation*. 1985;71:740-4.
24. Vasiljević JD, Popović ZB, Otasević P, Popović ZV, Vidaković R, Mirić M, et al. Myocardial fibrosis assessment by semiquantitative, point-counting and computer-based methods in patients with heart muscle disease: a comparative study. *Histopathology*. 2001;38:338-43.
25. Murray PA, Vatner SF. Reduction of maximal coronary vasodilator capacity in conscious dogs with severe right ventricular hypertrophy. *Circ Res*. 1981;48:25-33.
26. Rajappan K, Rimoldi OE, Dutka DP, Ariff B, Pennell DJ, Sheridan DJ, et al. Mechanisms of coronary microcirculatory dysfunction in patients with aortic stenosis and angiographically normal coronary arteries. *Circulation*. 2002;105:470-6.
27. Lamberts RR, Caldenhoven E, Lansink M, Witte G, Vaessen RJ, St Cyr JA, et al. Preservation of diastolic function in monocrotaline-induced right ventricular hypertrophy in rats. *Am J Physiol Heart Circ Physiol*. 2007;293:H1869-76.

ET/BS

28. Haddad F, Hunt SA, Rosenthal DN, Murphy DJ. Right ventricular function in cardiovascular disease, part I: anatomy, physiology, aging, and functional assessment of the right ventricle. *Circulation.* 2008;117:1436-48.
29. Burkhoff D, Mirsky I, Suga H. Assessment of systolic and diastolic ventricular properties via pressure-volume analysis: a guide for clinical, translational, and basic researchers. *Am J Physiol Heart Circ Physiol.* 2005;289:H501-12.
30. Faber MJ, Dalinghaus M, Lankhuizen IM, Steendijk P, Hop WC, Schoemaker RG, et al. Right and left ventricular function after chronic pulmonary artery banding in rats assessed with biventricular pressure-volume loops. *Am J Physiol Heart Circ Physiol.* 2006;291:H1580-6.
31. Dell'Italia LJ, Walsh RA. Application of a time varying elastance model to right ventricular performance in man. *Cardiovasc Res.* 1988;22:864-74.